

Published in final edited form as:

Nat Genet. 2018 February ; 50(2): 172–174. doi:10.1038/s41588-017-0022-7.

Loss-of-function variants in *ADCY3* increase risk of obesity and type 2 diabetes

Niels Grarup^{#1}, Ida Moltke^{#2}, Mette K. Andersen¹, Maria Dalby², Kristoffer Vitting-Seerup^{2,3}, Timo Kern¹, Yuvaraj Mahendran¹, Emil Jørsboe², Christina V. L. Larsen^{4,5}, Inger K. Dahl-Petersen⁴, Arthur Gilly⁶, Daniel Suveges⁶, George Dedoussis⁷, Eleftheria Zeggini⁶, Oluf Pedersen¹, Robin Andersson², Peter Bjerregaard^{4,5}, Marit E. Jørgensen^{4,5,8}, Anders Albrechtsen², and Torben Hansen^{1,9}

¹Novo Nordisk Foundation Center for Basic Metabolic Research, Faculty of Health and Medical Sciences, University of Copenhagen, Copenhagen, Denmark ²The Bioinformatics Centre, Department of Biology, University of Copenhagen, Copenhagen, Denmark ³Biotech Research & Innovation Centre (BRIC), University of Copenhagen, Copenhagen, Denmark ⁴National Institute of Public Health, University of Southern Denmark, Copenhagen, Denmark ⁵Greenland Centre for Health Research, University of Greenland, Nuuk, Greenland ⁶Department of Human Genetics, Wellcome Trust Sanger Institute, Hinxton, UK ⁷Department of Nutrition and Dietetics, Harokopio University of Athens, Athens, Greece ⁸Steno Diabetes Center Copenhagen, Gentofte, Denmark ⁹Faculty of Health Sciences, University of Southern Denmark, Odense, Denmark

These authors contributed equally to this work.

Abstract

We have identified a variant in adenylate cyclase 3 (*ADCY3*) associated with markedly increased risk of obesity and type 2 diabetes in the Greenlandic population. The variant disrupts a splice-acceptor site and carriers display decreased *ADCY3* RNA expression. Additionally, we observe an enrichment of rare *ADCY3* loss-of-function variants among type 2 diabetes patients in trans-ethnic

Users may view, print, copy, and download text and data-mine the content in such documents, for the purposes of academic research, subject always to the full Conditions of use:http://www.nature.com/authors/editorial_policies/license.html#terms

Corresponding authors: Torben Hansen, torben.hansen@sund.ku.dk, Anders Albrechtsen, albrecht@binf.ku.dk, Marit E. Jørgensen, marit.eika.joergensen@regionh.dk.

URLs

Accelerating Medicines Partnership Type 2 Diabetes Knowledge Portal: <http://www.type2diabetesgenetics.org/>

Genome Aggregation Database (gnomAD): <http://gnomad.broadinstitute.org/>

GTEX Portal: <https://www.gtexportal.org/>

FastQC: <http://www.bioinformatics.babraham.ac.uk/projects/fastqc/>

Contributions

T.H. and A.A. conceived and headed the project. I.M. and A.A. designed the statistical setup for the association testing, while T.H., N.G., M.K.A. and O.P. designed the experimental setup for the DNA extraction, genotyping and sequencing. M.E.J. and P.B. were PIs of the population studies in Greenland, and together with C.V.L.L., and I.K.D.-P. they provided the Greenlandic samples, collected and defined the phenotypes and provided context of these samples. I.M., N.G., E.J. and A.A. performed the association analyses. T.K. and Y.M. designed the experimental setup for RNA extraction and sequencing. A.G., D.S., G.D. and E.Z. performed the loss-of-function analysis in the Greek cohorts. K.V.S., M.D. and R.A. performed the RNA sequence analysis. N.G., I.M., M.K.A., A.A. and T.H. wrote the majority of the manuscript with input from all authors. All authors approved the final version of the manuscript.

Competing Financial Interests Statement

The authors report no competing financial interests.

cohorts. These findings provide novel information on disease etiology relevant for future treatment strategies.

Identification of homozygous loss-of-function mutations in humans may readily inform about the biological impact of specific genes and point to novel drug targets. We previously identified a loss-of-function variant in *TBC1D4* segregating at high frequency in the Greenlandic population displaying a high impact on risk of type 2 diabetes¹, confirming the advantage of studying the Greenlandic population due to its extreme demographic history². Motivated by this, we screened for novel loss-of-function variants in the exome sequencing data from 27 individuals in nine trios that were used to identify the causal *TBC1D4* loss-of-function variant¹. We identified 46 such variants (Supplementary Table 1) and intersected the location of these variants with loci known to associate with obesity or body mass index (BMI) (Supplementary Fig. 1). One of the variants, which was present in one copy in one of the trio's parents, was situated in a locus where a common non-coding variant has been shown to be associated with BMI in adults and children in genome-wide association studies (GWAS)^{3,4}. The variant (hg19: 2-25050478-C-T, c.2433-1G>A) is predicted to destroy a splice-acceptor site in exon 14 (NM_004036.4) (Fig. 1A) of *ADCY3*. For this reason, we investigated the specific variant further by genotyping it in two Greenlandic cohorts. This revealed an overall minor allele frequency of 2.3% in the Greenlandic study population ($N=4,038$, N -heterozygous=172, N -homozygous=7), and a frequency of 3.1% in the Inuit ancestry part of the population. Importantly, the seven homozygous carriers had a 7.3 kg/m² higher BMI ($P=0.00094$) compared with the remaining study population (Table 1). Interestingly, we also observed that three of the seven homozygous carriers had type 2 diabetes ($P=7.8\times 10^{-5}$, Table 1), while one had impaired fasting glucose and one impaired glucose tolerance. Notably, the association with type 2 diabetes remained significant after adjustment for BMI ($P=6.5\times 10^{-4}$), suggesting it is not simply mediated by increased BMI. The effects on BMI and type 2 diabetes were also observed, although with smaller effect sizes, when data were analyzed according to an additive genetic model (Table 1). However, when we compared the recessive and additive models with the full genotype model, we rejected the additive model (BMI: $P=0.002$; type 2 diabetes: $P=0.004$), but not the recessive model (BMI: $P=0.17$; type 2 diabetes: $P=0.095$). This suggests that the recessive model is appropriate for explaining the effect of the c.2433-1G>A variant.

To further characterize homozygous *ADCY3* c.2433-1G>A carriers in the Greenlandic cohorts, we analyzed a number of additional traits related to BMI and type 2 diabetes. The homozygous carriers had an 8.1 percentage points higher body fat percentage ($P=0.0024$) and a 17 cm larger waist circumference ($P=0.0017$). In addition, the homozygous carriers had nominally higher levels of fasting and 2-h plasma glucose after an oral glucose tolerance test ($P=0.022$ and $P=0.035$, respectively; Table 1). Finally, we also observed nominally significant effects on dyslipidemia and insulin resistance (Supplementary Table 2).

The c.2433-1G>A *ADCY3* variant was not observed in sequencing data of up to 138,000 individuals from non-Greenlandic populations collected by the Genome Aggregation Database Consortium⁵ (gnomAD). To generalize our findings to other populations, we therefore investigated the effect of loss-of-function variants in *ADCY3* more generally by

analyzing 18,176 samples with exome sequence data generated by the GoT2D, T2DGenes, SIGMA and LuCAMP consortia^{6,7,8}, which are available at the Accelerating Medicines Partnership Type 2 Diabetes Knowledge Portal (AMP-T2D). No homozygous *ADCY3* loss-of-function carriers were observed in this dataset, but the analysis included seven predicted *ADCY3* loss-of-function variants (Fig. 1A) observed in the heterozygous form in eight individuals, and we observed an enrichment of carriers among type 2 diabetes cases compared with non-diabetic controls (7/8,845 in cases, 1/9,323 in controls, OR 8.6, $P=0.044$, Supplementary Table 3-5). To further substantiate these findings, exome sequence data from 9,928 Finnish individuals from the METSIM cohort⁹ were screened for loss-of-function variants in *ADCY3*; however, none were identified (Markku Laakso, personal communication). Furthermore, we did not find any loss-of-function *ADCY3* variants in whole genome sequence data for 3,124 individuals from two Greek isolated populations as part of the HELIC study¹⁰. Finally, in up to 138,000 individuals in the gnomAD data, 48 predicted loss-of-function variants were found. All variants had minor allele frequency below 0.007% and only a single homozygous loss-of-function carrier was found for the African-specific *ADCY3* c.1072-1G>A variant. Since we cannot obtain phenotypic data for the gnomAD samples, we are unable to evaluate the impact of these variants on obesity and type 2 diabetes.

To investigate the functional impact of the *ADCY3* c.2433-1G>A variant, we performed deep RNA sequencing in leukocytes from 17 Greenlandic individuals (7 GG carriers, 6 GA carriers and 4 AA carriers). The RNA sequencing data confirmed that *ADCY3* was expressed in the wild type GG carriers and that exon 14 (NM_004036.4) of *ADCY3* was expressed and spliced in its canonical form (Supplementary Fig. 2A). The inclusion of exon 14 in the mature mRNA was further confirmed by RNA sequence data from adipose tissue of a healthy Caucasian female donor¹¹. Importantly, we found that the overall RNA expression level of *ADCY3* was severely decreased in the homozygous AA carriers, while the heterozygous GA carriers showed an intermediate expression level (Fig. 1B). The RNA sequencing data further confirmed that the predicted disruption of exon 14 splice-acceptor site by variant c.2433-1G>A has an impact on the molecular phenotype. Specifically, the data predict that two novel *ADCY3* isoforms are expressed in the variant carriers: one transcript isoform where exon 14 is skipped and an alternative splice-acceptor site at exon 15 is used and one transcript isoform in which the intron between exon 13 and exon 14 is retained (Supplementary Fig. 2B). We quantified these alternative splicing events by comparing the expression of the three predicted *ADCY3* isoforms using isoform fraction (IF) (Fig. 1C) and the percentage of spliced in (PSI) at the relevant splice sites (Supplementary Fig. 2B). Both analyses demonstrated that the homozygous AA carriers had severely affected splice pattern and mainly used intron retention (median IF 0.38, median PSI 75%) or exon skipping (IF 0.53, PSI 24%), while the wild type GG carriers had the canonical splice pattern (IF 0.88, PSI 87%). In all analyses, heterozygous carriers showed an intermediate level of alternative splicing (Fig. 1C; Supplementary Fig. 2B & C). Importantly, we predict the isoform with an intron retention to be sensitive to nonsense mediated decay due to a premature stop codon¹² (Fig. 1A). This predicted degradation naturally would lead to further reduction of *ADCY3* protein levels.

ADCY3 encodes an adenylate cyclase with a wide tissue distribution showing high levels in subcutaneous and visceral adipose tissue, intermediate levels in brain and rather low levels in pancreas and skeletal muscle in GTEx Project data. *ADCY3* catalyzes the synthesis of cAMP from ATP. cAMP is an essential second-messenger in intracellular signaling downstream of key metabolic mediators such as glucagon-like peptide 1, ghrelin and α -melanocyte stimulating hormone¹³, and cAMP signaling has been linked to control of adipose tissue development and function, as well as insulin secretion in beta cells¹⁴. In addition, mouse models have indicated that *ADCY3* plays an important role in the regulation of adiposity and glucose homeostasis. Hence, in mice, *Adcy3* haplo-insufficiency causes impaired insulin sensitivity and dyslipidaemia¹⁵, *Adcy3* gain-of-function protects from diet induced obesity¹⁶, and *Adcy3* knock-out mice show increased fat mass, hyperphagia, depression-like phenotypes, and leptin resistance^{17,18}. Possibly, leptin resistance occurs through disrupted cAMP signaling in primary cilia in hypothalamus affecting downstream signaling and morphology of the neurons^{17,18}. Interestingly, previously described syndromic forms of obesity, including Bardet-Biedl and Alström syndrome, are caused by altered function of primary cilia, and are besides from obesity characterized by diabetes¹⁹. Furthermore, common variation in *ADCY5*, a gene in the same family as *ADCY3*, is known to be associated with fasting plasma glucose levels and risk of type 2 diabetes²⁰.

In humans, common variants in the *ADCY3* locus have been associated with higher BMI^{3,4} and total as well as truncal fat mass²¹. Thus, the phenotype observed in Greenlandic homozygous loss-of-function carriers, characterized by truncal adiposity, insulin resistance, dyslipidemia and type 2 diabetes, is in accordance with and elaborates on the phenotype observed for GWAS-identified variants. Our findings for loss-of-function carriers implicate *ADCY3* as the causal transcript in the reported GWAS-identified locus, and coherent evidence from genetic and biological studies suggest that pharmacological modulation of this target may possibly be a valid future therapy for obesity and type 2 diabetes.

In conclusion, we identified an *ADCY3* loss-of-function variant in Greenlandic Inuit, which increases adiposity and risk of type 2 diabetes in homozygous carriers, and to a lesser extent in heterozygous carriers. Concomitantly, we detected decreased *ADCY3* RNA expression levels in homozygous carriers, and again to a lesser extent in heterozygous carriers. Furthermore, we show that the variant disrupts a splice-acceptor site, triggering exon skipping or intron retention, where the latter is predicted to confer nonsense-mediated decay. The association with type 2 diabetes was substantiated in trans-ethnic heterozygous carriers of rare *ADCY3* variants underlining the possible role of *ADCY3* as a future target for prevention and treatment of obesity and type 2 diabetes.

Online methods

Study samples

The Greenlandic samples are from two different cohorts: B99 ($N=1,401$) and Inuit Health in Transition (IHIT) ($N=3,115$), which were collected in Greenland as a part of general population health surveys conducted in 1999-2001 and 2005-2010, respectively^{22,23}. Two hundred and ninety-five individuals overlapped between the two cohorts and were assigned

to the B99 dataset. Clinical characteristics of the participants are shown in Supplementary Table 6.

Ethical considerations

The study has received ethics approval from the Commission for Scientific Research in Greenland (project 2011-13, ref. no. 2011-056978; and project 2013-13, ref.no. 2013-090702) and was conducted in accordance with the ethical standards of the Declaration of Helsinki, second revision. All participants gave written consent after being informed about the study both orally and in writing.

Phenotypic data

Height and weight were measured wearing light indoor clothes. Waist circumference was measured midway between the rib cage and the iliac crest and hip circumference at its maximum. Weight was measured on a standard electronic clinical scale. Fat percentage was calculated from bioimpedance measurements (Tanita TBF-300MA) in IHIT participants. Intraabdominal adipose tissue was assessed by ultrasonography, which is considered a valid and reproducible method compared with CT and MRI²⁴, using a 3.5 MHz transducer with the participant in supine position and at the end of a normal expiration. Tests for intra- and inter-observer variation were performed in IHIT and were in the range of 1.9-5.6%²⁵. In IHIT, all participants underwent an oral glucose tolerance test (OGTT). In B99, participants above 24 years of age had fasting blood samples taken and participants above 35 years underwent an OGTT. At the baseline health examination, venous blood samples were drawn after an overnight fast of at least 8 hours. After this, participants received a standard 75-g OGTT, with blood samples drawn 2 hours after the glucose intake. Only fasting venous plasma glucose was measured in participants with known diabetes. Fasting and 2-hours (2-h) plasma glucose values were analyzed with the Hitachi 912 system (Roche Diagnostics, Mannheim, Germany). Fasting and 2-h serum insulin levels were analyzed by an immunoassay method excluding des-31,32 split products and intact proinsulin (AutoDELFIA; Perkin Elmer, Waltham, MA). Indices of insulin sensitivity and insulin secretion were derived from plasma glucose and serum insulin measures from the OGTT. Hepatic insulin sensitivity was estimated by the homeostasis model assessment (HOMA-IR = fasting glucose [mmol/L] × (fasting insulin [pmol/L]/6.945) / 22.5)²⁶ and by a peripheral insulin sensitivity index (ISI_{0,120}) calculated as: $ISI_{0,120} = ((75000 + (\text{fasting glucose}[\text{mmol/L}] \times 18 - 2\text{-h glucose} \times 18) \times 0.19 \times \text{weight} [\text{kg}]/120) / ((\text{fasting glucose}[\text{mmol/L}] \times 18 + 2\text{-h glucose}[\text{mmol/L}] \times 18) / 2)) / \log((\text{fasting insulin}[\text{pmol/L}]/6.945 + 2\text{-h insulin}[\text{pmol/L}]/6.945)/2)$ ²⁷. Analyses of quantitative glycemic traits were performed excluding individuals with previously diagnosed diabetes. Individuals taking lipid-lowering medication were removed in analysis of fasting serum lipids. Dichotomous glycaemia variables were constructed to test for association with type 2 diabetes classified according to the World Health Organization criteria²⁸.

Identification and selection of loss-of function variants to study

To identify the novel loss-of-function variants in the Greenlandic population we used the exome data from 27 Greenlandic individuals in nine trios presented previously¹. In this dataset, we identified 46 loss-of-function variants, which were not present in dbSNP

(version 138 and below) and that were not present in NHLBI Exome Sequencing Project (ESP) (Supplementary Table 1). We then used the GWAS catalogue (downloaded January 2013) to assign known associations to the loci with the loss-of-function variants using associations with P -values of less than 10^{-7} . Finally, we selected the variants with known associations to obesity or BMI for further study. This selection procedure left us with one predicted loss-of-function variant, *ADCY3* c.2433-1G>A (Supplementary Fig. 1). This variant is located in *ADCY3* and was present in a single parent in one of the nine trios in heterozygous form.

Genotype data

Subsequently, we genotyped *ADCY3* c.2433-1G>A in the two Greenlandic cohorts, IHIT and B99, using KASP Genotyping Assay (LGC Genomics, Hoddlesdon, UK). Genotyping call rate was 99.2% and no mismatches were observed in 362 samples genotyped in duplicate. For the association testing, we used quality filtered MetaboChip genotype data to base our genetic similarity matrix estimates on. The genotyping and quality filtering of the MetaboChip data has been described in detail earlier²⁹. The filtered MetaboChip dataset contains data from 2,791 individuals from IHIT and 1,336 individuals from B99 and we have *ADCY3* c.2433-1G>A genotyping data for 4,038 of these individuals, 2,779 from IHIT and 1,259 from B99.

Association testing and replication

Greenlandic cohorts—To test for association between the *ADCY3* variant and the different phenotypes of interest we used a linear mixed model, implemented in the software GEMMA³⁰, in order to account for relatedness and admixture¹. For each phenotype, GEMMA was applied to data from the subset of individuals across the two cohorts with information available about that specific phenotype. The genetic similarity matrix required as input to GEMMA was estimated from MetaboChip genotype data¹. For each phenotype, we performed two association tests: a test where we assumed a recessive effect model and a test where we assumed an additive effect model. All tests were performed with sex, age and cohort included as covariates. An additional analysis also included BMI as covariate. Before all tests for association with quantitative traits, we quantile transformed the phenotype data to a normal distribution separately for each sex, which resulted in the results reported as β_{SD} , se_{SD} and P . However, to get effect sizes in the units the traits were measured in, we also performed the analyses without transforming the phenotype data, which resulted in the results reported as β . For the binary trait, type 2 diabetes, we did not perform any transformation and the test results are reported as β and P .

To assess the appropriateness of the recessive effect model and the additive effect model for BMI and type 2 diabetes we compared each of these effects models against a full genotype model, where each of the three genotypes have an independent effect. To do this, we used the same linear model framework as we did for the association tests. These additional tests were only performed in the IHIT cohort because there were no homozygous carriers in B99, which in practice means the tests cannot be performed if B99 is included.

Accelerating Medicines Partnership Type 2 Diabetes Knowledge Portal (AMP-T2D)—Data from AMP-T2D generated as part of the GoT2D, T2DGenes, SIGMA and LuCAMP consortia^{6,7,8} were queried for association between a burden of loss-of-function variants in *ADCY3* and type 2 diabetes. The data contained 18,869 samples with exome sequence data of which 18,176 samples were informative for type 2 diabetes. Samples originated from five ancestries (6,356 Europeans, 5,722 Hispanic, 2,199 South Asians, 2,158 East Asians and 1,741 African Americans). Variants annotated as stop-gained, frameshift or in a splice adapter/donor site were considered loss-of-function. Burden association analyses were performed with each individual coded as carrying a loss-of-function variant or not. We used logistic regression and adjusted for principal components 1-4 as well as age and sex by including these as covariates. We also analyzed all other genes with at least five loss-of-function variants with at least one mutation carrier for each variant. Only loss-of-function variants with a minor allele frequency (MAF) <5% were used. This analysis showed that there is no general inflation in the test statistic (Supplementary Fig. 3).

Greek isolated populations—As part of the HELIC study¹⁰, 1,642 samples from the Pomak villages in Northern Greece and 1,482 samples from the Mylopotamos villages in Crete were sequenced at an average depth of 18.6x and 22.5x, respectively using the HiSeqX platform. Adapter-ligated libraries were amplified by 6 cycles of PCR and subjected to DNA sequencing according to manufacturer's instructions. GVCFs were created for 200 equally sized chunks using GATK HaplotypeCaller v3.5, combined into batches of 150 samples using GATK CombineGVCFs and called using GATK GenotypeGVCFs. Variant-level QC was performed using GATK VQSR v.3.5.

Estimation of admixture proportions, ancestral allele frequencies and relatedness

For the Greenlanders, all admixture proportions were obtained from ref. 1. To estimate the ancestral Inuit allele frequencies for the *ADCY3* variant we performed maximum likelihood estimation using the likelihood model from ADMIXTURE³¹ with the admixture proportions fixed and including only genotype data from the variant of interest. To achieve the maximum likelihood estimates we applied an EM-algorithm. We estimated relatedness using relateAdmix³² based on the estimated admixture proportions. None of the seven homozygous carriers are closely related (2nd-degree or closer), however one pair may be first cousins with an estimated kinship coefficient of 0.08.

RNA sequencing analysis

RNA sequencing was performed on leukocytes from 17 Greenlandic individuals (7 GG carriers, 6 GA carriers and 4 AA carriers). The total RNA was extracted from 2.5 mL of peripheral blood with the PAXGene Blood miRNA Kit (Qiagen) according to the manufacturer's protocol, and subjected to on-column DNase I treatment with RNase-free Dnase (Qiagen). The RNA quality and purity were checked using Agilent 2100 Bioanalyzer (Agilent RNA 6000 Nano Kit) and NanoDropTM, respectively.

The RNA sequencing library was prepared following the instructions of the TruSeq RNA Sample Prep Kit v2 (Illumina): For mRNA isolation and fragmentation 200 ng of total RNA was purified by oligo-dT beads before fragmentation with Elute, Prime, Fragment Mix.

First-strand cDNA was generated using First Strand Mix and SuperScript II (Invitrogen) reverse transcription master mix (reaction condition: 25°C for 10 min; 42°C for 50 min; 70°C for 15 min). The second-strand was synthesized by adding Second Strand Master Mix (16°C for 1h). The fragmented cDNA was end-repaired and purified with Ampure XP Beads (AGENCOURT). A-Tailing Mix was added and incubated (37°C for 30 min). For the adapter ligation, Adenylate 3'Ends DNA, RNA Index Adapter and Ligation Mix, were mixed and incubated (30°C for 10 min). End-repaired DNA was purified with Ampure XP Beads (AGENCOURT). Several rounds of PCR amplification with PCR Primer Cocktail and PCR Master Mix were performed to enrich the cDNA fragments. The PCR products were purified with Ampure XP Beads (AGENCOURT). The average molecule length was measured using the Agilent 2100 bioanalyzer instrument (Agilent DNA 1000 Reagents), and by real-time quantitative PCR (TaqMan Probe). The qualified libraries were amplified on cBot to generate the cluster on the flowcell (TruSeq PE Cluster Kit V3-cBot-HS, Illumina). The amplified flow cell was sequenced paired-end on the HiSeq 4000 System (TruSeq SBS KIT-HS V3, Illumina).

The obtained RNA-seq libraries, as well as one RNA-seq library from adipose tissue of a healthy Caucasian female¹¹ were processed by Trimmomatic v 0.32.33 trimming the reads using HEADCROP:11 LEADING:22 SLIDINGWINDOW:4:22 MINLEN:25. Quality of all libraries were checked with FastQC, before and after trimming. Trimmed reads were mapped un-stranded to the human reference genome (hg19) using Hisat2 v2.0.1-beta34 with splice site information from GENCODE v19.35 and set to annotate properly paired reads as those with a minimum insert size from 0 to 1000 nucleotides. Sashimi plots³⁶ were generated from the IGV genome browser³⁷. PSI was calculated as $r_{\text{exon:intron}} / (r_{\text{exon:intron}} + r_{\text{exon:exon}})$ where r is the number of reads indicating the different splice patterns. $r_{\text{exon:intron}}$ was obtained by extracting relevant GENCODE v19.35 exon:intron boundaries +/- 3 nucleotides. Reads mapping to these regions were quantified using featureCounts from the R package Rsubread³⁸ specifying countChimericFragments=FALSE and minOverlap=6, ensuring that reads map across the exon boundary. $r_{\text{exon:exon}}$ was calculated by running featureCounts with the juncCounts=TRUE parameter. Plots were made using ggplot2. For transcript quantification, we constructed a gtf file containing three versions of GENCODE v19 transcript ENST00000260600.5, the longest transcript for ADCY3. The corresponding genomic sequences were extracted using Cufflinks gffread tool³⁹ and a Salmon index was built using Salmon v0.8.2.40. Untrimmed fastq files were used to quantify the resulting transcripts using Salmon v0.8.2⁰. Calculations of isoform fractions and prediction of functional consequences, were done with the R package IsoformSwitchAnalyzeR¹² using standard parameters except the filtering where geneExpressionCutoff = 1, and isoformExpressionCutoff = 0.5, and keepIsoformInAllConditions=TRUE, supplied to the preFilter() function. Hmmer scan v.3.1.41 was used to predict pfamA protein domains as described in the IsoformSwitchAnalyzeR vignette and integrated into the analysis by the analyzePFAM() function. The functional consequences of isoform switches was predicted by IsoformSwitchAnalyzeR's analyzeSwitchConsequences() function.

Data availability

The Greenlandic exome sequencing and RNA sequencing data have been deposited at the European Genome-phenome Archive (<https://www.ebi.ac.uk/ega/home>) under accession number EGAS00001002727. Trans-ethnic data analyzed in the project are available at <http://www.type2diabetesgenetics.org/gene/geneInfo/ADCY3> upon registration at the website. Repositories of genetic variation and gene expression were queried at <http://gnomad.broadinstitute.org/> and <https://www.gtexportal.org/>, respectively.

Supplementary Material

Refer to Web version on PubMed Central for supplementary material.

Acknowledgements

We gratefully acknowledge the participants in the Greenlandic health surveys. We thank Dr. Flannick, Broad Institute, US for help with obtaining the AMP-T2D exome sequencing data. The Novo Nordisk Foundation Center for Basic Metabolic Research is an independent Research Center at the University of Copenhagen partially funded by an unrestricted donation from the Novo Nordisk Foundation (www.metabol.ku.dk). This project was also funded by the Danish Council for Independent Research (Sapere Aude DFF-Ung Eliteforsker grant 11-120909 from FSS to I.M.; DFF-4090-00244 from FNU to I.M.; Sapere Aude DFF-Forskingsleder 6108-00038B from FNU to R.A., DFF-4181-00383 to A.A.), the Steno Diabetes Center Copenhagen (www.steno.dk), Simon Fougnier Hartmanns Familiefond to N.G., the Lundbeck foundation (R215-2015-4174) to A.A., the Novo Nordisk Foundation (NNF15OC0017918 to N.G.; NNF16OC0019986 to N.G.; NNFCC0018486 to T.H.) and the European Research Council (ERC) under the European Union's Horizon 2020 research and innovation programme (grant agreement no. 638173) to R.A.. The Greenlandic health surveys (IHIT and B99) were supported by Karen Elise Jensen's Foundation, the Department of Health in Greenland, NunaFonden, Medical Research Council of Denmark, Medical Research Council of Greenland, and the Commission for Scientific Research in Greenland.

References

- Moltke I, et al. *Nature*. 2014; 512:190–3. [PubMed: 25043022]
- Pedersen CT, et al. *Genetics*. 2017; 205:787–801. [PubMed: 27903613]
- Speliotes EK, et al. *Nat Genet*. 2010; 42:937–48. [PubMed: 20935630]
- Warrington NM, et al. *Int J Epidemiol*. 2015; 44:700–12. [PubMed: 25953783]
- Lek M, et al. *Nature*. 2016; 536:285–91. [PubMed: 27535533]
- Fuchsberger C, et al. *Nature*. 2016; 536:41–7. [PubMed: 27398621]
- The Sigma Type Diabetes Consortium. et al. *JAMA*. 2014; 311:2305–14. [PubMed: 24915262]
- Lohmueller KE, et al. *Am J Hum Genet*. 2013; 93:1072–86. [PubMed: 24290377]
- Laakso M, et al. *J Lipid Res*. 2017; 58:481–493. [PubMed: 28119442]
- Panoutsopoulou K, et al. *Nat Commun*. 2014; 5:5345. [PubMed: 25373335]
- Liu Y, et al. *PLoS One*. 2013; 8:e66883. [PubMed: 23826166]
- Vitting-Seerup K, Sandelin A. *Mol Cancer Res*. 2017; 15:1206–1220. [PubMed: 28584021]
- Xu TR, Yang Y, Ward R, Gao L, Liu Y. *Cell Signal*. 2013; 25:2413–23. [PubMed: 23917208]
- Yang H, et al. *J Mol Endocrinol*. 2016; 57:R93–R108. [PubMed: 27194812]
- Tong T, et al. *Sci Rep*. 2016; 6:34179. [PubMed: 27678003]
- Pitman JL, et al. *PLoS One*. 2014; 9:e110226. [PubMed: 25329148]
- Wang Z, et al. *PLoS One*. 2009; 4:e6979. [PubMed: 19750222]
- Chen X, et al. *Biol Psychiatry*. 2016; 80:836–848. [PubMed: 26868444]
- Vaisse C, Reiter JF, Berbari NF. *Cold Spring Harb Perspect Biol*. 2017; 9
- Dupuis J, et al. *Nat Genet*. 2010; 42:105–116. [PubMed: 20081858]
- Tachmazidou I, et al. *Am J Hum Genet*. 2017; 100:865–884. [PubMed: 28552196]
- Bjerregaard P, et al. *Int J Circumpolar Health*. 2003; 62(Suppl 1):3–79. [PubMed: 14527126]

23. Bjerregaard, P. 2011. http://www.si-folkesundhed.dk/upload/inuit_health_in_transition_Greenland_methods_5_2nd_revision.pdf
24. Philipsen A, et al. PLoS One. 2015; 10:e0123062. [PubMed: 25849815]
25. Jørgensen ME, et al. Diabetes Care. 2013; 36:2988–94. [PubMed: 23656981]
26. Matthews DR, et al. Diabetologia. 1985; 28:412–9. [PubMed: 3899825]
27. Gutt M, et al. Diabetes Res Clin Pract. 2000; 47:177–84. [PubMed: 10741566]
28. World Health Organization Study Group. World Health Organization; Geneva: 1999.
29. Andersen MK, et al. PLoS Genet. 2016; 12:e1006119. [PubMed: 27341449]
30. Zhou X, Stephens M. Nat Genet. 2012; 44:821–4. [PubMed: 22706312]
31. Alexander DH, Novembre J, Lange K. Genome Res. 2009; 19:1655–64. [PubMed: 19648217]
32. Moltke I, Albrechtsen A. Bioinformatics. 2014; 30:1027–28. [PubMed: 24215025]
33. Bolger AM, Lohse M, Usadel B. Bioinformatics. 2014; 30:2114–20. [PubMed: 24695404]
34. Kim D, Langmead B, Salzberg SL. Nat Methods. 2015; 12:357–60. [PubMed: 25751142]
35. Harrow J, et al. Genome Res. 2012; 22:1760–74. [PubMed: 22955987]
36. Katz Y, et al. Bioinformatics. 2015; 31:2400–2. [PubMed: 25617416]
37. Robinson JT, et al. Nat Biotechnol. 2011; 29:24–6. [PubMed: 21221095]
38. Liao Y, Smyth GK, Shi W. Bioinformatics. 2014; 30:923–30. [PubMed: 24227677]
39. Trapnell C, et al. Nat Biotechnol. 2010; 28:511–5. [PubMed: 20436464]
40. Patro R, Duggal G, Love MI, Irizarry RA, Kingsford C. Nat Methods. 2017; 14:417–419. [PubMed: 28263959]
41. Punta M, et al. Nucleic Acids Res. 2012; 40:D290–301. [PubMed: 22127870]

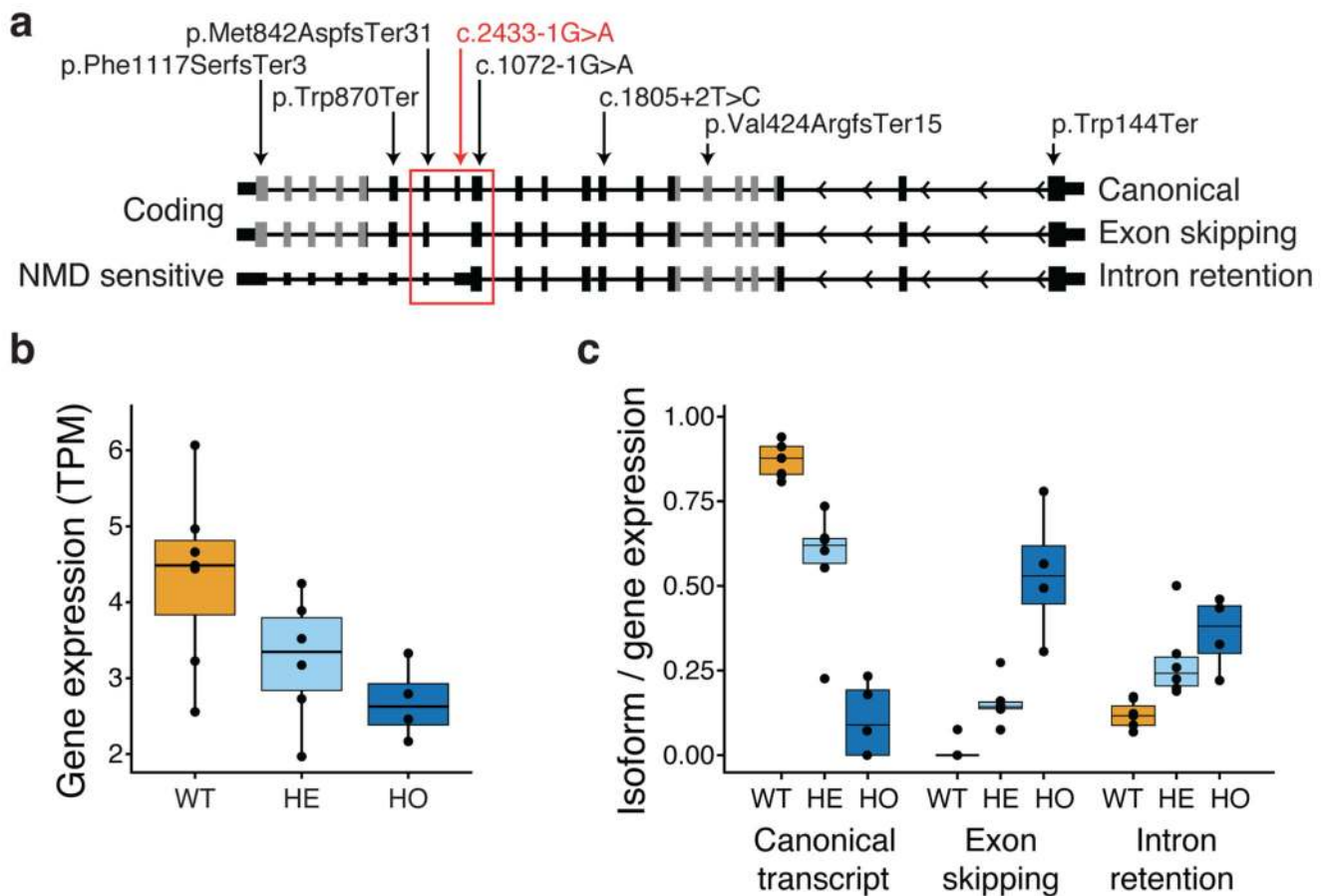


Figure 1. *ADCY3* isoforms, observed loss-of-function variants and functional consequences based on RNA sequencing of leukocytes from 17 Greenlandic individuals.

a. Schematic representation of *ADCY3* displaying the three relevant transcript isoforms and their predicted functional consequences annotated to the left (“Coding” or “nonsense mediated decay (NMD) sensitive”). The exons that correspond to the protein domain, Guanylate cyclase, are shown as gray filled boxes, while the rest of the exons are shown as black filled boxes. The red square encapsulates the exons affected by the Greenlandic *ADCY3* c.2433-1G>A variant. The locations of the identified loss-of-function variants in *ADCY3* in the Greenlandic and trans-ancestry cohorts are shown with arrows in red and black, respectively. Variants were annotated to canonical transcript *ADCY3*-201 (NM_004036) except c.1072-1G>A, which is annotated to alternative transcript *ADCY3*-202 (NM_001320613). **b.** *ADCY3* Transcripts Per Million (TPM) normalized gene expression, stratified according to *ADCY3* c.2433-1G>A variant genotype groups (WT, wild type; HE, heterozygous; and HO, homozygous). **c.** *ADCY3* transcript isoform fractions for the three quantified isoforms, the canonical isoform, the novel exon skipping and intron retention splice version stratified according to *ADCY3* c.2433-1G>A variant genotype groups. Number of individuals in each group in b and c are: WT: 7 GG carriers, HE: 6 GA carriers, and HO: 4 AA carriers. The lower and upper hinges of boxes in b and c correspond to the first and third quartiles of data, respectively, while the middle line is the median and

the whiskers extends to the largest and smallest data points no further away than 1.5 times the interquartile range.

Table 1
Association of *ADCY3* c.2433-1G>A with obesity and type 2 diabetes-related traits in Greenlandic cohorts.

Trait	N	Recessive model				Additive model			
		β_{SD}	se _{SD}	β	P	β_{SD}	se _{SD}	β	P
Type 2 diabetes (cases/ controls)	301/2,585			0.50	7.8×10⁻⁵			0.081	0.0014
BMI (kg/m ²)	4,001	1.2	0.36	7.3	0.00094	0.18	0.075	1.00	0.017
Fat percentage (%)	2,701	1.1	0.35	8.1	0.0024	0.18	0.078	1.56	0.024
Fasting plasma glucose (mmol/L)	3,622	0.77	0.34	0.76	0.022	0.12	0.072	0.11	0.088
2-h plasma glucose (mmol/L)	3,387	0.73	0.35	2.3	0.035	0.13	0.073	0.45	0.090

Results are shown for a recessive and an additive genetic model. β_{SD} and se_{SD} are the effect size and standard error estimated using quantile transformed values of the trait (except for the binary trait type 2 diabetes) and β is the effect size estimated using untransformed values. The *P*-values were obtained from the analyses of quantile transformed traits (except for the binary trait type 2 diabetes). *P*-values shown have not been corrected for multiple testing and nominally significant *P*-values are highlighted in bold.